

Lattice calculation of α_s in momentum scheme

Ph. Boucaud^a, J.P. Leroy^a, J. Micheli^a, O. Pène^a, and C. Roiesnel^b

July 7, 2018

^aLaboratoire de Physique Théorique et Hautes Energies¹
 Université de Paris XI, Bâtiment 211, 91405 Orsay Cedex, France

^b Centre de Physique Théorique² de l'Ecole Polytechnique
 F91128 Palaiseau cedex, France

Abstract

We compute the flavorless running coupling constant of QCD from the three gluon vertex in the (regularisation independent) momentum subtraction renormalisation scheme. This is performed on the lattice with high statistics. The expected color dependence of the Green functions is verified. There are significant $O(a^2\mu^2)$ effects which can be consistently controlled. Scaling is demonstrated when the renormalisation scale is varied between 2.1 GeV and 3.85 GeV. Scaling when the lattice spacing is varied is very well satisfied. The resulting flavorless conventional two loop $\Lambda_{\overline{\text{MS}}}^{(c)}$ is estimated to be, respectively for the MOM and $\widetilde{\text{MOM}}$ scheme, 361(6) MeV and 345(6) MeV, while the three loop results are, depending on β_2 : $\Lambda_{\overline{\text{MS}}}^{(3)} = (412 - 59 \frac{\beta_2}{\beta_{2,\overline{\text{MS}}}} \pm 6 \text{ MeV})$ and $\Lambda_{\overline{\text{MS}}}^{(3)} = (382 - 46 \frac{\beta_2}{\beta_{2,\overline{\text{MS}}}} \pm 5 \text{ MeV})$. A preliminary computation of β_2 in the $\widetilde{\text{MOM}}$ scheme leads to $\Lambda_{\overline{\text{MS}}}^{(3)} = 303(5) \frac{a^{-1}(\beta=6.0)}{1.97 \text{ GeV}}$ MeV.

LPTHE Orsay-98/49
 hep-ph/9810322

¹Laboratoire associé au Centre National de la Recherche Scientifique - URA D00063

² Unité Mixte de Recherche C7644 du Centre National de la Recherche Scientifique

The non-perturbative calculation of the running coupling constant of QCD is certainly one very important problem. This program has been performed using the Schrödinger functional [1], the heavy quark potential [2]-[3], the Wilson loop [4], the Polyakov loop [5] and the three gluon coupling [6]. The latter method is the one we will follow in the present letter. The principle of the method is quite simple since it consists in following the steps which are standard in perturbative QCD in the momentum subtraction scheme. One usually uses as a subtraction point for the three gluon vertex function an Euclidean point with symmetric momenta: $p_1^2 = p_2^2 = p_3^2 \equiv \mu^2$.

In [6] this non-perturbative minimum subtraction calculation has been performed, but using an asymmetric subtraction point $p_1^2 = p_3^2 \equiv \mu^2, p_2 = 0$. The presence of a vanishing momentum induces some subtleties which will be discussed later. The running coupling constant computed in [6] shows a signal of perturbative scaling at large scale.

In this letter we perform the same program with symmetric subtraction points, which is the genuine non-perturbative momentum subtraction scheme. We also repeat the work done in [6]. The whole calculation is achieved with a larger statistics, a check of finite volume effects, and a check of scaling when the lattice spacing a is varied.

In section 1 the general principle of the method is recalled and the systematic construction of the symmetric momentum points is summarized. In section 2 the lattice calculation is described including the checks of color behaviour, of finite volume effects, and the discussion of $O(a^2\mu^2)$ and three loop effects. Both the scaling in μ and in a are demonstrated. In section 3 we compare our result for $\Lambda_{\overline{MS}}$ with other lattice approaches and conclude.

1 Computing α_s from non-perturbative Green functions

In this section we describe the general method used to compute α_s and Λ_{QCD} in the continuum, assuming one is able to compute the Euclidean Green functions of QCD in the Landau gauge. The lattice aspect will be treated in the next section. The principle of the method is exactly the standard textbook [7] one, generalized to non-perturbative QCD [6].

The Euclidean two point Green function in momentum space writes in the Landau Gauge:

$$G_{\mu_1\mu_2}^{(2) a_1 a_2}(p, -p) = G^{(2)}(p^2) \delta_{a_1 a_2} \left(\delta_{\mu_1 \mu_2} - \frac{p_{\mu_1} p_{\mu_2}}{p^2} \right) \quad (1)$$

where a_1, a_2 are the color indices ranging from 1 to 8.

The three-gluon Green function is equal to the color tensor³ $f^{a_1 a_2 a_3}$ times a momentum dependent function which may be expressed [8] as a sum of scalar functions multiplied by tensors: $\sum A_i(p_1^2, p_2^2, p_3^2) T_{i; \mu_1 \mu_2 \mu_3}$, the $T_{i; \mu_1 \mu_2 \mu_3}$ being built up from $\delta_{\mu_j \mu_k}$ and momenta. In general there is some arbitrariness in choosing the tensor basis. One of these may be taken to be the tree level three-gluon vertex, projected transversally to the momenta (Landau gauge):

$$T_{\mu_1 \mu_2 \mu_3}^{tree} = [\delta_{\mu'_1 \mu'_2} (p_1 - p_2)_{\mu'_3} + \text{cycl. perm.}] \prod_{i=1,3} \left(\delta_{\mu'_i \mu_i} - \frac{p_i \mu'_i p_i \mu_i}{p_i^2} \right) \quad (2)$$

while the choice of the other tensors in the tensor basis will be explained below in the particular cases. Calling $G^{(3)}(p_1^2, p_2^2, p_3^2)$ the scalar function which multiplies the tensor (2), the renormalised coupling constant in the considered scheme is given by [6]

$$g_R(\mu^2) = \frac{G^{(3)}(p_1^2, p_2^2, p_3^2) Z_3^{3/2}(\mu^2)}{G^{(2)}(p_1^2) G^{(2)}(p_2^2) G^{(2)}(p_3^2)} \quad (3)$$

where

$$Z_3(\mu^2) = G^{(2)}(\mu^2) \mu^2 \quad (4)$$

and μ^2 is the renormalisation scale which will be specified in each scheme.

The justification of eq. (3) is standard: the momentum scheme fixes the renormalisation constants so that the two-point and three-point renormalised Green functions at the renormalisation point take their tree value with the only substitution of the bare coupling by the renormalised one. In particular the renormalised $G_R^{(2)}(p^2)$ takes its tree value, $1/p^2$, at $p^2 = \mu^2$, which fixes the field renormalisation constant (4). The renormalised coupling constant is then defined so that the three-point Green function is equal to the bare tree level one (with the substitution of g_0 by g_R) at the symmetric Euclidean point $p_1^2 = p_2^2 = p_3^2 \equiv \mu^2$.

At the symmetric point only two independent tensors exist in Landau gauge⁴, which we choose to be:

$$G_{\mu_1 \mu_2 \mu_3}^{(3) a_1 a_2 a_3}(p_1, p_2, p_3) = f^{a_1 a_2 a_3} \left[G^{(3)}(\mu^2, \mu^2, \mu^2) T_{\mu_1 \mu_2 \mu_3}^{tree} + \right. \\ \left. H^{(3)}(\mu^2, \mu^2, \mu^2) \frac{(p_1 - p_2)_{\mu_3} (p_2 - p_3)_{\mu_1} (p_3 - p_1)_{\mu_2}}{\mu^2} \right] \quad (5)$$

with T^{tree} defined in (2). To project out $G^{(3)}(\mu^2, \mu^2, \mu^2)$ we contract with the appropriate tensor:

$$G^{(3)}(\mu^2, \mu^2, \mu^2) f^{a_1 a_2 a_3} = \frac{1}{18 \mu^2} G_{\mu_1 \mu_2 \mu_3}^{(3) a_1 a_2 a_3}(p_1, p_2, p_3)$$

³In general schemes and gauges the $d^{a_1 a_2 a_3}$ tensor should also be considered, but not in our case as we shall see.

⁴Notice that in the Landau gauge the transversality condition with respect to the external momenta, reduces the number of independent tensors as compared to a general covariant gauge.

$$\left[T_{\mu_1\mu_2\mu_3}^{tree} + \frac{(p_1 - p_2)_{\mu_3}(p_2 - p_3)_{\mu_1}(p_3 - p_1)_{\mu_2}}{2\mu^2} \right] \quad (6)$$

In the following we will call this momentum configuration the ‘‘symmetric’’ one, and this defines the MOM scheme.

We have also considered the $\widetilde{\text{MOM}}$ scheme defined by subtracting the vertex function at the asymmetric Euclidean point $p_1^2 = p_3^2 \equiv \mu^2$, $p_2 = 0$. In Landau gauge there remains only one tensor, the one in (2), which simplifies:

$$G_{\mu_1\mu_2\mu_3}^{(3) a_1 a_2 a_3}(p, 0, -p) = 2f^{a_1 a_2 a_3} p_{\mu_2} \left[\delta_{\mu_1\mu_3} - \frac{p_{\mu_1} p_{\mu_3}}{\mu^2} \right] G^{(3)}(\mu^2, 0, \mu^2) \quad (7)$$

and the scalar factor is extracted via

$$G^{(3)}(\mu^2, 0, \mu^2) f^{a_1 a_2 a_3} = \frac{1}{6\mu^2} G_{\mu_1\mu_2\mu_3}^{(3) a_1 a_2 a_3}(p, 0, -p) \delta_{\mu_1\mu_3} p_{\mu_2} \quad (8)$$

In the following we will call this momentum configuration the ‘‘asymmetric’’ one.

Some caution is in order for the latter asymmetric configuration. From (1) it is clear that

$$G^{(2)}(p^2) \delta_{a_1 a_2} = \frac{1}{3} \sum_{\mu} G_{\mu\mu}^{(2) a_1 a_2}(p, -p) \quad (9)$$

for any non vanishing value of the momentum. But when the momentum vanishes, the term $p_{\mu} p_{\mu} / p^2$ is undetermined. It could seem quite natural to follow by continuity formula (9). On the other hand since only the tensor $\delta_{\mu\nu}$ is defined for zero momentum, $G_{\mu\nu}^{(2)}(0, 0) = \delta_{\mu\nu} G^{(2)}(0)$ leads to replacing the factor 1/3 by 1/4. Indeed, the Landau gauge condition does not eliminate global gauge transformations, and one additional degree of freedom is left at zero momentum. This theoretical issue is delicate but it is perfectly obvious that the numerical results favor in a dramatic way the factor 1/4. When using the factor 1/3 no sign of perturbative scaling can be seen. The factor 1/4 was used in [6] and we will follow the same recipe.

1.1 Computing Λ_{QCD}

The conventional two-loop $\Lambda^{(c)}$ is obtained in any scheme from $\alpha(\mu^2) \equiv g_R(\mu^2)^2 / (4\pi)$ by

$$\Lambda^{(c)} \equiv \mu \exp \left(\frac{-2\pi}{\beta_0 \alpha(\mu^2)} \right) \times \left(\frac{\beta_0 \alpha(\mu^2)}{4\pi} \right)^{-\frac{\beta_1}{\beta_0^2}} \quad (10)$$

where

$$\mu \frac{\partial \alpha}{\partial \mu} = -\frac{\beta_0}{2\pi} \alpha^2 - \frac{\beta_1}{4\pi^2} \alpha^3 - \frac{\beta_2}{64\pi^3} \alpha^4 - \dots \quad (11)$$

$\beta_0 = 11$, $\beta_1 = 51$ and β_2 is scheme dependent ($\beta_{2, \overline{\text{MS}}} = 2857$). Integrating exactly eq. (11) expanded up to order α^{n+1} , and imposing the asymptotic limit

$\Lambda^{(n)}/\Lambda^{(c)}(\alpha) \rightarrow 1$ when $\alpha \rightarrow 0$, leads to the definition

$$\Lambda^{(2)} \equiv \left(1 + \frac{\beta_1 \alpha}{2\pi\beta_0}\right)^{\left(\frac{\beta_1}{\beta_0^2}\right)} \Lambda^{(c)}(\alpha) \quad (12)$$

at two loop and to the three loop $\Lambda^{(3)}$:

$$\Lambda^{(3)} \equiv \Lambda^{(c)}(\alpha) \left(1 + \frac{\beta_1 \alpha}{2\pi\beta_0} + \frac{\beta_2 \alpha^2}{32\pi^2\beta_0}\right)^{\frac{\beta_1}{2\beta_0^2}} \times \exp\left\{\frac{\beta_0\beta_2 - 4\beta_1^2}{2\beta_0^2\sqrt{\Delta}} \left[\arctan\left(\frac{\sqrt{\Delta}}{2\beta_1 + \beta_2\alpha/4\pi}\right) - \arctan\left(\frac{\sqrt{\Delta}}{2\beta_1}\right)\right]\right\} \quad (13)$$

when $\Delta \equiv 2\beta_0\beta_2 - 4\beta_1^2 > 0$.

One simple criterium has been proposed in [6] to exhibit perturbative scaling: when plotting (10) as a function of μ perturbative scaling implies that Λ should become constant for large enough μ . We will thus try to fit each of the formulae (10), (12), (13), expressed in terms of our measured $\alpha(\mu)$, as a constant. All these formulae converge to the same Λ when $\alpha \rightarrow 0$. But since our fits are for α in the range of 0.3 - 0.5, and since they do not have the same dependence on α they should not all fit our data. However, as we shall see, within our errors, acceptable fits are possible with (10), and (13) varying β_2 on a wide range. This is due to the fact that, even with our rather large statistics, the three loop effect, being only logarithmic, does not modify strongly enough the variation of $\Lambda(\alpha)$ in our fitting range although the resulting fitted Λ depends significantly on the formula used and on β_2 . In other words we have different acceptable fits, with slightly different slopes in μ , which lead asymptotically, when $\alpha \rightarrow 0$, to significantly different Λ 's. There results a systematic error which cannot be fully eliminated until β_2 is really computed.

Notwithstanding this problem, we believe that the possibility to fit several of these formulae by a constant on a large range of μ and with small statistical errors, is an indication that perturbative scaling has been reached. In other words, our data show that the uncertainty is of logarithmic type (higher loops), but there is no room for significant power corrections. To study power corrections, one has to consider with care lower scales [12], and we plan to do that in a forthcoming publication [14].

In order to compare different schemes, it is standard to translate the results into the $\overline{\text{MS}}$ scheme. Once known in any scheme, a one loop computation is enough to yield Λ_{QCD} in any other scheme [10], [11]. From [10] and [6] we get for zero flavors

$$\Lambda_{\text{MOM}} = 3.334\Lambda_{\overline{\text{MS}}}, \quad \Lambda_{\widetilde{\text{MOM}}} = \exp(70/66) \simeq 2.888\Lambda_{\overline{\text{MS}}}. \quad (14)$$

1.2 Momenta

In a finite hypercubic volume the momenta are the discrete set of vectors

$$p_\mu = 2\pi n_\mu / L \quad (15)$$

where n_μ are integer and L is the lattice size. The isometry group for momenta is generated by the four reflections $p_\mu \rightarrow -p_\mu$ for $\mu = 1, \dots, 4$ and the permutations between the four directions such as $p_x \leftrightarrow p_y$. Altogether this group has $2^4 4! = 384$ elements. We use fully this symmetry in order to increase the statistics. The functions $G^{(2)}(p^2)$ and $G^{(3)}(p^2, 0, p^2)$ in eqs (1) and (7) are systematically symmetrized over the momenta lying on one given group orbit. The number of distinct momenta in an orbit is 384 or a divisor of 384 (when the momentum is invariant by some subgroup).

In the case of $G^{(3)}(p^2, p^2, p^2)$ in eq. (5) we furthermore symmetrize over the 6 permutations of external legs (Bose symmetry). The number of elements in an orbit will be $6 \times 384 = 2304$ or one of its divisors.

1.3 Triplets of external momenta

We build all triplets of momenta up to some maximum value of the momentum to be specified later.

In the asymmetric case, there are as many triplets as momenta. For every integer number there exists at least one orbit of the isometry group with $n_\mu n^\mu$ equal to that integer. The number of elements is often a much smaller number than 384: 1, 8, 16, 24, 64, etc.

In the symmetric case, $n_\mu n^\mu$ has to be an *even* number: $n_1^2 = n_2^2 = (n_1 + n_2)^2$, where the subindices label the external particles, and consequently, $n_{1\mu} n_2^\mu = -n_1^2/2$ being an integer, n_1^2 is even. It happens that for every even integer, we have found at least one orbit. The number of elements in one orbit is often a large number, 2304 and 1152 are frequent, 576 and 192 are less. Notwithstanding these larger sets, the statistical noise will turn out to be larger in the symmetric case than in the asymmetric one. Let us give some examples of symmetric triplets: for $n^2 = 2$: (1100)(0 - 110)(-10 - 10) and its 192 transformed by the isometry-Bose group; for $n^2 = 4$: (2000)(-1111)(-1 - 1 - 1 - 1) and its 192 transformed. For $n^2 = 16$: (4000)(-2222)(-2 - 2 - 2 - 2) its 192 transformed. For $n^2 = 18$ there are 6 orbits, for example (4110)(-1 - 2 - 32)(-312 - 2) and its 2304 transformed, (3300)(-1 - 232)(-2 - 1 - 3 - 2) and its 1152 transformed, etc.

2 Lattice calculation of α_s and Λ_{QCD} .

2.1 The calculation.

The calculation has been performed on a QUADRICS QH1, with hypercubic lattices of 16^4 and 24^4 sites at $\beta = 6.0$, 24^4 at $\beta = 6.2$ (all three with 1000 configurations) and 32^4 at $\beta = 6.4$ (100 configurations), combining the Metropolis and the overrelaxation algorithms.

The configurations have been transformed to the Landau gauge by a combination of overrelaxation algorithm and Fourier acceleration. We end when $|\partial_\mu A_\mu|^2 < 10^{-12}$ and when the spatial integral of A_0 is constant in time to better than 10^{-5} .

We define

$$A_\mu(x + \hat{\mu}/2) = \frac{U_\mu(x) - U_\mu^\dagger(x)}{2ia g_0} - \frac{1}{3} \text{Tr} \left(\frac{U_\mu(x) - U_\mu^\dagger(x)}{2ia g_0} \right) \quad (16)$$

where $\hat{\mu}$ indicates the unit lattice vector in the direction μ and g_0 is the bare coupling constant, and compute the n-point Green functions in momentum space from

$$G_{\mu_1 \mu_2 \dots \mu_n}^{(n) a_1 a_2 \dots a_n}(p_1, p_2, \dots p_n) = \langle A_{\mu_1}^{a_1}(p_1) A_{\mu_2}^{a_2}(p_2) \dots A_{\mu_n}^{a_n}(p_n) \rangle \quad (17)$$

where $p_1 + p_2 + \dots + p_n = 0$, $\langle \rangle$ indicates the Monte-Carlo average and where

$$A_\mu^a(p) = \frac{1}{2} \text{Tr} \left[\sum_x A_\mu(x + \hat{\mu}/2) \exp(ip(x + \hat{\mu}/2)) \lambda^a \right] \quad (18)$$

λ^a being the Gell-Mann matrices and the trace being taken in the 3×3 color space.

We have computed the Fourier transforms up to a maximum momentum of $\simeq 3$ GeV at $\beta = 6$, and $\simeq 4.2$ GeV at $\beta = 6.2$ and $\beta = 6.4$. These maxima correspond to $n^2 \equiv n_\mu n^\mu \leq 16$ for $(\beta, V) = (6.0, 16^4)$ and ≤ 36 for all the other cases.

2.2 Check of the color dependence

From the color structure of QCD we expect the two point Green functions to be proportional to the color tensor $\delta_{a_1 a_2}$. This is indeed the case to an accuracy of the order of 1 %. Furthermore one can prove from gauge symmetry (global and local) and Bose symmetry that the three point Green functions have to be proportional to $f^{a_1 a_2 a_3}$ in the MOM and $\widetilde{\text{MOM}}$ schemes. This is indeed the case, but the errors now depend on the momentum. For small values of n^2 the agreement is of a few percent. The errors increase with n^2 and when n^2 reaches the 30's the error reaches 100 %. This is an indication that the large momenta are grieved by noise. Luckily this caution is necessary only for the very few largest values of n^2 that we have considered. Indeed we will exclude the points $n^2 > 30$ from our fits. In order to reduce the noise we work from now on with color averaged Green functions: $\frac{1}{24} G^{(3) a_1 a_2 a_3} f^{a_1 a_2 a_3}$ and $\frac{1}{8} G^{(2) a_1 a_2} \delta_{a_1 a_2}$.

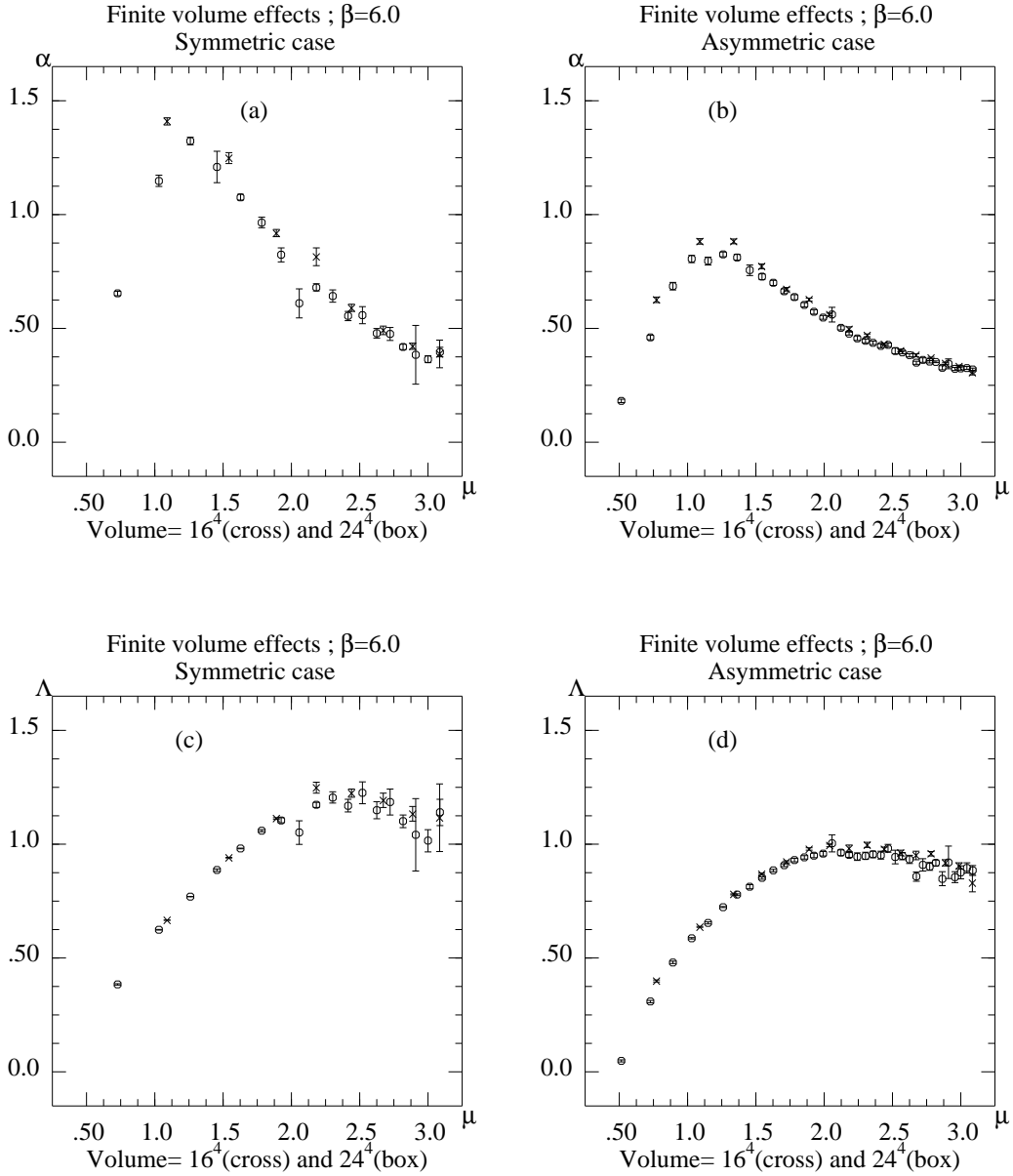


Figure 1: Comparison between the volumes of 16^4 and 24^4 at $\beta = 6$ for the coupling $\alpha(\mu)$ (figs. a and b), $\Lambda_{\text{MOM}}^{(c)}$ (fig. c) and $\Lambda_{\text{MOM}}^{(c)}$ (fig. d). No “sinus improvement” has been applied here.

β	Volume	range (GeV)	$a\Lambda_{\overline{\text{MS}}}^{(c)}/(a\sqrt{\sigma})$ sym	$a\Lambda_{\overline{\text{MS}}}^{(c)}/(a\sqrt{\sigma})$ asym
6.0	16^4	2.1 - 3.0	0.845(25)	0.809(22)
6.0	24^4	2.1 - 3.0	0.811(24)	0.784(23)
6.2	24^4	2.1 - 3.85	0.861(27)	0.805(21)
6.4	32^4	2.1 - 3.85	0.861(45)	0.793(27)

Table 1: Ratios $a\Lambda_{\overline{\text{MS}}}^{(c)}/(a\sqrt{\sigma})$ for different values of β after “sinus improvement” as explained in section 2.4. The numbers for $a\sqrt{\sigma}$ are taken from [2]. The errors on $a\Lambda$ and $a\sqrt{\sigma}$ have been combined in quadrature. The scaling invariance is particularly striking especially at constant physical volume, i.e. comparing lines 1,3,4.

2.3 Finite volume effects

The finite volume effects can be checked by a comparison of the two calculations at $\beta = 6.0$, Fig 1. For relatively small μ , close to the maximum of α , there is a visible decrease of α when the volume is increased.

For larger μ , the volume dependence is still visible, but reduced to a few percent. Comparing the values of Λ fitted in the asymptotic region given in table 1, one finds

$$\Lambda_{sym}(24)/\Lambda_{sym}(16) = 0.96 \pm 0.02, \quad \Lambda_{asym}(24)/\Lambda_{asym}(16) = 0.97 \pm 0.02 \quad (19)$$

which indicates that the finite volume effect affects moderately the asymptotic estimate of Λ . More study is needed to quantify precisely this effect. Still, from gross estimates, our largest physical volume, $\beta = 6.0$, 24^4 , lies presumably within 5% above the infinite volume limit.

2.4 Scaling in μ and $O(a^2p^2)$ effects

Figs. 1(a,b) show the shape of $\alpha(\mu)$. The same shape is seen for the other β 's. In fact $\alpha(\mu)$ scales in a to a very good accuracy. We keep this study for another publication [14].

Turning to the scaling in μ , we see from figs 1(c,d) that both Λ 's do not really show plateaus at large momentum: they go through a maximum around 2 GeV and fall down later on. Our study shows that this feature cannot be cured simply by a three loop effect. Using eq. (13) with different values for β_2 cannot lead to acceptable plateaus for all lattice spacings. Since the fall at large μ is

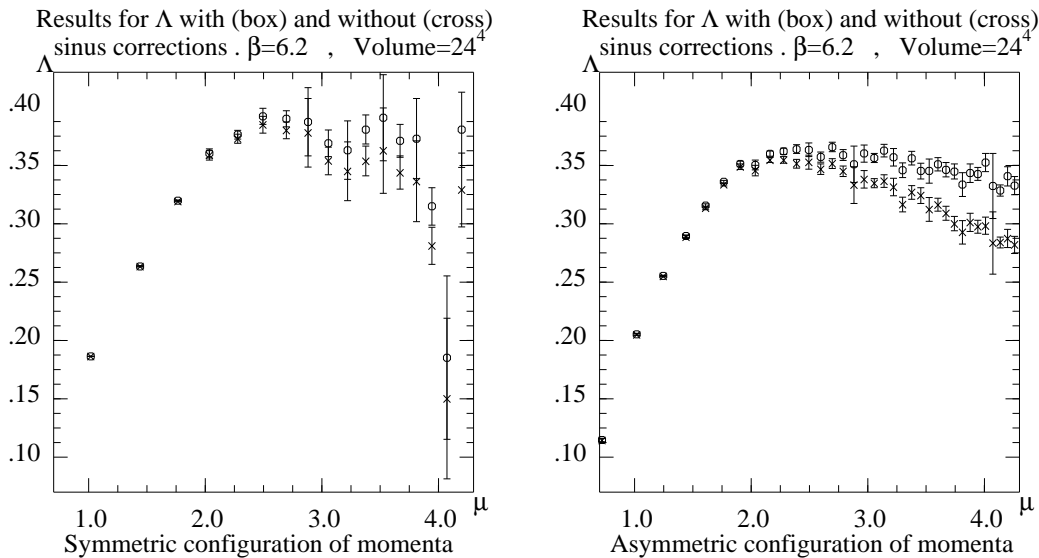


Figure 2: The effect of the “sinus improvement” on $\Lambda_{\text{MS}}^{(c)}$ is illustrated in the case of the 1000 configurations at $(\beta, V) = (6.2, 24^4)$. A similar improvement can be seen in all cases.

observed systematically, beyond statistical errors, but decreases when β increases, we conjecture that we deal with an $O(a^2 p^2)$ effect.

We have successfully tried a correction which will be described now. It starts from the remark that in the lattice Landau gauge, obtained by minimizing $\sum_{\mu,x} \text{Tr}[1 - U_\mu(x)]$, $p_\mu A_\mu^a(p)$ does not vanish while $\tilde{p}_\mu A_\mu^a(p)$ does, when $A_\mu^a(p)$ is defined from eq (18) and where

$$\tilde{p}_\mu = \frac{2}{a} \sin\left(\frac{ap_\mu}{2}\right). \quad (20)$$

The latter momentum differs from the one in (15) by $O(a^2 p^2)$: $\tilde{p}_\mu \simeq p_\mu(1 - \frac{1}{24} a^2 p_\mu^2)$. It results that the lattice two point Green function is not really proportional to the tensor in (1) but to the tensor deduced from (1) with p_μ substituted by \tilde{p}_μ , [9].

We perform a similar change in the tensors used to extract α . The projectors in (6) and (8) have been normalized to give 1 when contracted to the tensors which multiply $G^{(3)}$ in (5) and (7) respectively. Assuming that the lattice calculations is such as to produce the tensors in (5) and (7) with p_μ substituted by \tilde{p}_μ , there would be a bias in our formulae (6) and (8). Indeed the contraction of the “tilded” tensors in (5) and (7) with the tensors in (6) and (8) is smaller than one and decreases with increasing p . We tentatively correct the bias by dividing the result in (3) by this factor smaller than one. We shall refer to this as the “sinus improvement”.

For brevity we only show $(\beta, V) = (6.2, 24^4)$ in fig. 2. The improvement of

β	6.0	6.0	6.2	6.4
Volume (lat)	16^4	24^4	24^4	32^4
Volume (phys)	$(1.63 \text{ fm})^4$	$(2.44 \text{ fm})^4$	$(1.75 \text{ fm})^4$	$(1.75 \text{ fm})^4$
range (GeV)	2.1 - 3.0	2.1 - 3.0	2.1 - 3.85	2.1 - 3.85
$\Lambda_{\overline{\text{MS}}}^{(c)}$ (MeV)	356(4)	345(6)	354(5)	353(11)
χ^2/dof	1.44	1.12	1.87	1.13
$\Lambda_{\overline{\text{MS}}}^{(2)}$ (MeV)	401(5)	389(7)	397(6)	394(14)
χ^2/dof	3.13	1.66	5.99	1.43
$\Lambda_{\overline{\text{MS}}}^{(3)}$ (MeV)	314(3)	303(5)	313(4)	312(9)
χ^2/dof	1.30	1.29	1.02	1.18
unimpr. $\Lambda_{\overline{\text{MS}}}^{(c)}$ (MeV)	332(4)	324(6)	338(5)	344(11)
χ^2/dof	6.51	3.71	12.3	1.58

Table 2: Fitted $\Lambda_{\overline{\text{MS}}}$ for the *asymmetric* momentum configurations. The “sinus improved” Λ ’s is used except for the last two lines. To exhibit the a -scaling we use the ratios $\sqrt{\sigma_0}(a\Lambda_{\overline{\text{MS}}}/(a\sqrt{\sigma}))$ with $\sigma_0 = 445 \text{ MeV}$ as justified in section 2.6. $\Lambda^{(3)}$ has been computed with $\beta_2 = 1.69\beta_{2,\overline{\text{MS}}} \simeq 4824$. The χ^2/dof ’s correspond to the fit in the preceding line.

the plateaus is dramatic. The large μ fall has been considerably reduced. The improvement is confirmed by a reduction of the χ^2 per degree of freedom from exceedingly large values to acceptable ones, see tables 2 and 3.

Of course, this is only an ad hoc $O(a^2p^2)$ improvement, by no way rigorous and systematic. Fitting directly a corrective term of the form $1 - ca^2p^2$ leads also to drastically improved χ^2 with best values of c in reasonable agreement with the “sinus improvement” ($c \sim 1/24$). It should be stressed that the sinus improvement, and the $1 - ca^2p^2$ fits yield very similar values of Λ . We may thus conclude that the $O(a^2p^2)$ systematic error on Λ is moderate after “sinus improvement”.

2.5 Three loop effect.

A final source of systematic uncertainty comes from our ignorance of β_2 in the MOM scheme. From a preliminary perturbative calculation [15] in the $\widetilde{\text{MOM}}$ scheme we get $\beta_2 \simeq 4824$. On the other hand we unsuccessfully tried to fix β_2 non-perturbatively from our asymptotic fits. The ratio $\Lambda^{(3)}/\Lambda^{(c)}$, eqs (10)-(13), drops from 1 when α increases, the drop increasing with β_2 . As a result, the fitted value for $\Lambda^{(3)}$ will decrease as β_2 increases. Simultaneously the shape of the

β	6.0	6.0	6.2	6.4
Volume (lat)	16^4	24^4	24^4	32^4
Volume (phys)	$(1.63 \text{ fm})^4$	$(2.44 \text{ fm})^4$	$(1.75 \text{ fm})^4$	$(1.75 \text{ fm})^4$
range (GeV)	2.1 - 3.0	2.1 - 3.0	2.1 - 3.85	2.1 - 3.85
$\Lambda_{\overline{\text{MS}}}^{(c)}$ (MeV)	376(6)	361(6)	381(8)	383(20)
χ^2/dof	0.38	1.06	0.89	1.50
$\Lambda_{\overline{\text{MS}}}^{(2)}$ (MeV)	442(9)	425(10)	444(12)	455(30)
χ^2/dof	3.22	1.58	1.89	1.06
$\Lambda_{\overline{\text{MS}}}^{(3)}$ (MeV)	326(5)	311(5)	329(7)	330(16)
χ^2/dof	0.19	1.25	1.12	1.79
unimpr. $\Lambda_{\overline{\text{MS}}}^{(c)}$ (MeV)	364(6)	351(7)	372(8)	380(21)
χ^2/dof	2.99	1.49	1.69	1.24

Table 3: This table is the analog of table 2 but for the *symmetric* momentum configurations.

plateaus are modified. In principle, the requirement of an acceptable χ^2 might have restricted the admissible domain for β_2 . Unhappily our preliminary analysis did not turn out to be so restrictive. Only for β_2 below $0.5\beta_{2,\overline{\text{MS}}}$ does the χ^2 become prohibitive, see for example the $\beta_2 = 0$ case ($\Lambda^{(2)}$) in tables 2 and 3. It might look strange that $\Lambda^{(c)}$ fits well while $\Lambda^{(2)}$ does not, both being two-loop formulae. In fact $\Lambda^{(c)}$ is only an approximate two-loop formula which can be proven to be very close to $\Lambda^{(3)}$ with $\beta_2 \simeq 8\frac{\beta_1^2}{\beta_0} \simeq 0.66\beta_{2,\overline{\text{MS}}}$.

We therefore cannot do better in the MOM scheme, at present, than to provide fits of $\Lambda^{(3)}$ as a function of β_2 . For comparison we also provide the same analysis in the $\overline{\text{MOM}}$ scheme. The maximum value for β_2 which we consider is $\beta_2 = 2\beta_{2,\overline{\text{MS}}} = 5714$ since, for such a large value, the term $\propto \alpha^4$ in the β function (11) is of the same order as the term $\propto \alpha^3$ for our range of α . If β_2 was larger than that, the perturbative expansion would be dubious, and the evidence for perturbative scaling shown by our data would appear as a miraculous fake.

2.6 Scaling in a

The ‘‘sinus improved’’ Λ ’s exhibit a very clear scaling when μ varies above 2.1 GeV, as can be seen from the quality of the plateaus in figs 2 and 3 and from the χ^2 per d.o.f. In this subsection we want to study further the scaling when β , i.e. a , is varied.

Since Λ depends linearly on a^{-1} , the consistency of our fits can only be checked through a spacing independent ratio. We use the ratios $a\Lambda/(a\sqrt{\sigma})$, see table 1, where $a\sqrt{\sigma}$ is the central value of string tension computed in [2].

In order to write Λ in physical units we then multiply all ratios by one global scale factor: $\sqrt{\sigma_0} = 445$ MeV tuned to the central value of a very recent fit [13] from the K^* mass: $a^{-1}(\beta = 6.2) = 2.75(18)$ GeV. We take the central value: $a^{-1}(\beta = 6.2) = 2.75$ GeV, whence $a^{-1}(\beta = 6.0) = 1.966$ GeV and $a^{-1}(\beta = 6.4) = 3.664$ GeV.

This leads to the plots in fig. 3. The presence of nice plateaus is striking. We fit the average Λ on these plateaus, for scales never smaller than 2.1 GeV, and as high as allowed by lattice effects. The results are presented in tables 1, 2 and 3. The fits for $\Lambda^{(c)}$ and for a large range of $\Lambda^{(3)}$ yield a χ^2 per degree of freedom smaller than 1.5. *Scaling in the lattice spacing is striking*, especially for those lattice parameters which correspond to a similar physical volume of $\simeq (1.7 \text{ fm})^4$, i.e. $(\beta, V) = (6.0, 16^4), (6.2, 24^4)$ and $(6.4, 32^4)$. They average to:

$$\Lambda_{\overline{\text{MS}}}^{(c)} = 378(6) \text{ MeV (symmetric)} \quad \Lambda_{\overline{\text{MS}}}^{(c)} = 355(4) \text{ MeV (asymmetric)}$$

$$\Lambda_{\overline{\text{MS}}}^{(3)}(\beta_2 = 1.69 \beta_{2\overline{\text{MS}}} = 4824) = \begin{cases} 327(5) \text{ MeV (symmetric)} \\ 313(3) \text{ MeV (asymmetric)} \end{cases} \quad (21)$$

where the errors are only statistical. $\beta_2 = 4824$ results from our preliminary calculation [15] in the asymmetric scheme. For comparison we provide the result with the same β_2 in the symmetric case. The result at the larger volume of $\simeq (2.44 \text{ fm})^4$, $(\beta, V) = (6.0, 24^4)$, presumably close to the infinite volume limit (section 2.3), is:

$$\Lambda_{\overline{\text{MS}}}^{(c)} = 361(6) \text{ MeV (symmetric)} \quad \Lambda_{\overline{\text{MS}}}^{(c)} = 345(6) \text{ MeV (asymmetric)}$$

$$\Lambda_{\overline{\text{MS}}}^{(3)}(\beta_2 = 1.69 \beta_{2\overline{\text{MS}}} = 4824) = \begin{cases} 311(5) \text{ MeV (symmetric)} \\ 303(5) \text{ MeV (asymmetric)} \end{cases} \quad (22)$$

Varying β_2 we find acceptable χ^2 's from $\beta_2 \approx 0.5\beta_{2\overline{\text{MS}}} = 1428$ up to beyond $2\beta_{2\overline{\text{MS}}} = 5714$ which we take as the maximum perturbatively consistent value, see section 2.5. In this range of β_2 the fitted $\Lambda^{(3)}$ have, to a surprisingly good approximation, a linear dependence on β_2 . We provide the result in the next section.

Finally it is worth mentioning that we have also checked scaling of α in a over the whole range in μ , including the small values. We leave this point for a forthcoming publication [14]

3 Discussions and conclusions

There is scaling, as can be seen first from the plateaus of Λ as a function of the momentum scale μ , and second from the striking agreement of the runs for different β 's. We now quote our final results from our largest physical volume,

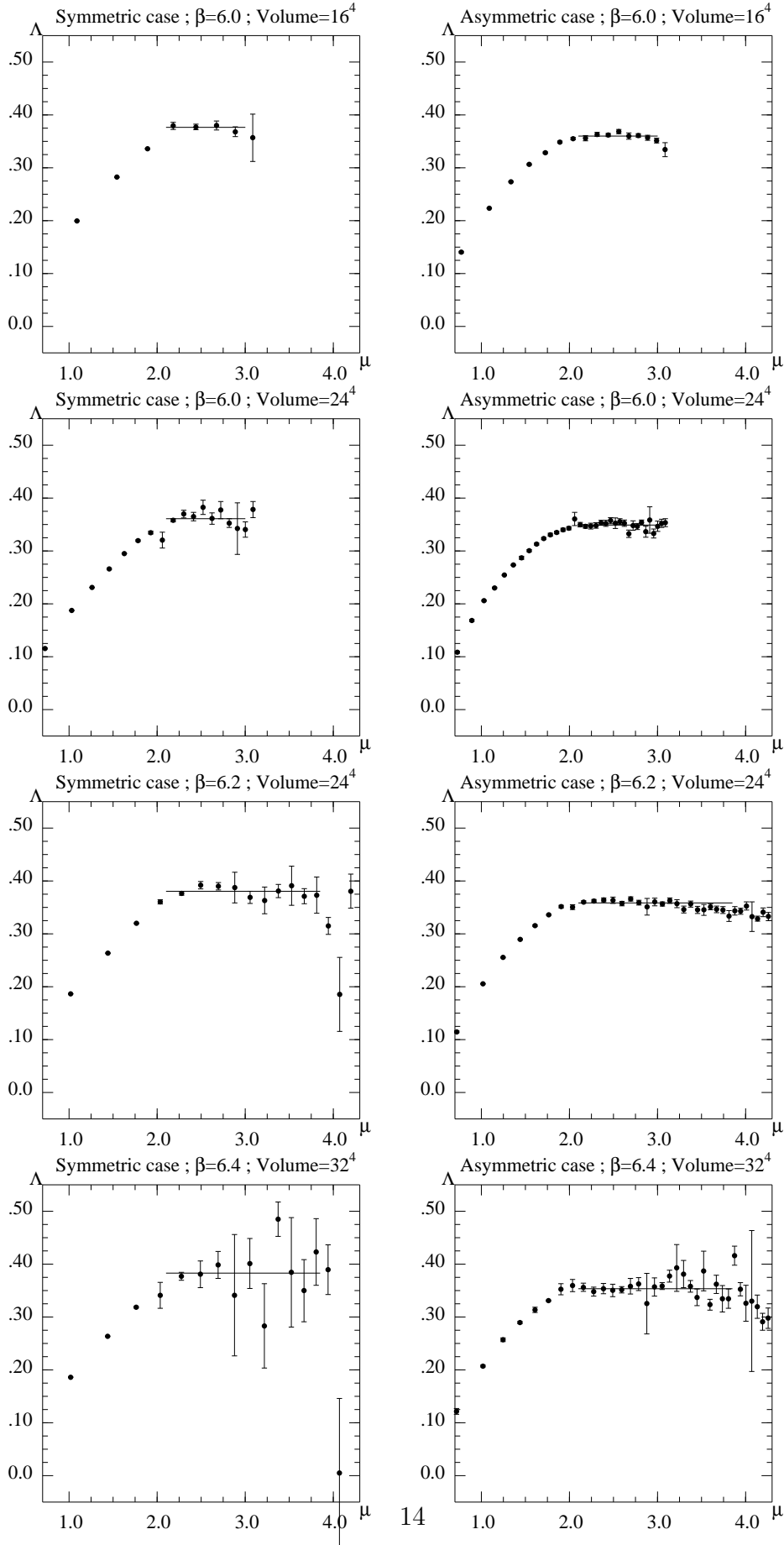


Figure 3: The fits for $a\Lambda_{\text{MS}}^{(c)}/(a\sqrt{\sigma_0})\sqrt{\sigma_0}$ (with $\sqrt{\sigma_0} = 445$ MeV), including the

$(\beta, V) = (6.0, 24^4)$, which we estimate to give values of Λ less than 5% from the infinite volume limit.

The analysis for symmetric momentum configurations is better grounded theoretically since it avoids the delicate problem of zero momentum. On the other hand, this analysis is noisier than the asymmetric one which exhibits beautiful plateaus. The good agreement of these two analyses allows a sort of reciprocal support.

Several other lattice estimates of Λ have been performed. The ALPHA collaboration, [1], quotes $\Lambda_{\overline{\text{MS}}} = 251(21)$ MeV. Other results are 244(8) MeV [2], $293(18)_{63}^{25}$ MeV [3], 340(50) [6].

Our results for Λ happen to be very sensitive to the three loop effect but β_2 cannot be fitted non perturbatively from our data. A wide range, $0.5\beta_{2,\overline{\text{MS}}} = 1428 \leq \beta_2 \leq 2\beta_{2,\overline{\text{MS}}} = 5714$ is allowed, in which the three loop $\Lambda^{(3)}$ can be approximated by the following formulae:

$$\Lambda_{\overline{\text{MS}}}^{(3)} = \left[\left(412 - 59 \frac{\beta_2}{\beta_{2,\overline{\text{MS}}}} \pm 6 \right) \text{MeV} \right] \frac{a^{-1}(\beta = 6.0)}{1.97\text{GeV}} \text{ (symmetric)}$$

$$\Lambda_{\overline{\text{MS}}}^{(3)} = \left[\left(382 - 46 \frac{\beta_2}{\beta_{2,\overline{\text{MS}}}} \pm 5 \right) \text{MeV} \right] \frac{a^{-1}(\beta = 6.0)}{1.97\text{GeV}} \text{ (asymmetric)} \quad (23)$$

Comparing the results in both schemes seems to indicate that the β_2 's in MOM and $\widetilde{\text{MOM}}$ schemes are not too different. A calculation of β_2 in the MOM scheme would be most welcome.

Our preliminary computation of β_2 in the $\widetilde{\text{MOM}}$ scheme, [15], uses the results of [16] and yields a value of $\beta_{2,\widetilde{\text{MOM}}} \simeq 1.69 \beta_{2,\overline{\text{MS}}} \simeq 4824$. *Our final result is then*

$$\Lambda_{\overline{\text{MS}}}^{(3)} = (303 \pm 5 \text{ MeV}) \frac{a^{-1}(\beta = 6.0)}{1.97\text{GeV}} \text{ (asymmetric)} \quad (24)$$

Acknowledgements.

These calculations were performed on the QUADRICS QH1 located in the Centre de Ressources Informatiques (Paris-sud, Orsay) and purchased thanks to a funding from the Ministère de l'Education Nationale and the CNRS. We are specially indebted to Francesco Di Renzo, Claudio Parrinello and Carlotta Pittori for thorough discussions which helped initiating this work We acknowledge Damir Becirevic, Konstantin Chetyrkin, Yuri Dokshitzer, Ulrich Ellwanger, Gregory Korchemsky and Alfred Mueller for several inspiring comments.

References

- [1] M. Lüscher, Talk given at the 18th International Symposium on Lepton-Photon Interactions, Hamburg, 28 July-1 August 1997; Lecture at l'Ecole des Houches, August 26-29 1997; M.Lüscher, R.Sommer, P.Weisz and U. Wolf, Nucl. Phys. **B413**(1994)481.
- [2] G.S. Bali and K. Schilling Phys. Rev. **D47** (1993) 661.
- [3] G.S.Bali, In Prodvino 1993, Problems on high energy physics and field theory 147-163, hep-lat/9311009.
- [4] G.P.Lepage and P. Mackenzie, Phys. Rev. Lett. **D48**(1992)2250.
- [5] G. de Divitiis et al, Nucl. Phys. **B433**(1995)390; **B437**(1995)447.
- [6] B. Alles, D. Henty, H. Panagopoulos, C. Parrinello, C. Pittori, D.G. Richards, Nucl. Phys. **B502** (1997) 325; C. Parrinello Nucl. Phys. Proc. Suppl. **63** (1998) 245; B. Alles, D. Henty, H. Panagopoulos, C. Parrinello, C. Pittori, IFUP-TH-23-96, hep-lat/9605033.
- [7] H.D. Politzer, Phys. Reports **14C** (1974) 141.
- [8] J.S. Ball and T-W. Chiu, Phys. Rev. **D22** (1980) 2550.
- [9] D.Zwanziger, Nucl Phys. **B364** (1991)127.
- [10] W.Celmaster and R.J.Gonsalves Phys. Rev. **D20** (1979) 1420.
- [11] A.Billoire Phys. Lett. **B104** (1981) 472.
- [12] G. Burgio, F. Di Renzo, C. Parrinello and C. Pittori, LTH 417, hep-ph/9808258.
- [13] D. Becirevic et al. LPTHE-Orsay 98/33, hep-lat/9809129.
- [14] D. Becirevic et al. in preparation.
- [15] Ph. Boucaud et al. in preparation
- [16] A.I.Davydychev, P.Osland and O.V.Tarasov Phys. Rev. **D58** (1998) 036007.